Bull. Mater. Sci., Vol. 38, No. 1, February 2015, pp. 101–104. © Indian Academy of Sciences.

Magnetocaloric response of $La_{0.70}Ca_{0.1}Sr_{0.2}Fe_{0.1}Mn_{0.9}O_3$ pervoskite for magnetic refrigeration

M S ANWAR, FAHEEM AHMED and BON HEUN KOO*
College of Science and General Studies, Alfaisal University, Riyadh 11533, Saudi Arabia

MS received 20 February 2014; revised 29 April 2014

Abstract. **The complex magnetic materials $La_{0.70}Ca_{0.1}Sr_{0.2}Fe_{0.1}Mn_{0.9}O_3$ (LCSFMO) and $La_{0.70}Ca_{0.1}Sr_{0.2}MnO_3$ (LCSMO), applicable for the magnetic cooling, have been explored. The X-ray diffraction patterns show that these samples are in single phase with rhombohedral structure. A remarkable decrease in the Curie temperature from 346 to 223 K was observed for 10% of Fe doping at Mn-site in the LCSMO sample. The substitution of Mn by Fe results in a combination of doping disorder, a site-percolation and Mn–Fe super-exchange interactions, which suppresses the ferromagnetism. The maximum magnetic entropy change of 1.53 J kg^{-1} K^{-1} with field variation of 3 T was obtained for the LCSFMO sample. The relative cooling power (RCP) ∼120 J kg^{-1} was found for an applied magnetic field of 3 T. The comparable magnetic entropy change and RCP values suggested that the studied samples have potential as a refrigerant for cooling applications.**

Keywords. **Magnetic materials; oxides; microstructure; SEM; magnetocaloric effect.**

1. Introduction

In recent times, the magnetic refrigeration at room temperature has been received increasing attention against the well-established gas refrigeration technology.[1–3] The magnetic materials that can display a large magnetocaloric effect (MCE) were reported as candidate materials for magnetic refrigeration.[4–7] Rare-earth manganites of the $A_{1-x}B_xMnO_3$ type (where A = La, Pr, Nd, etc. and B = Ca, Sr, Ba, etc.) have been explored in the last decade, owing to their good magnetocaloric response at various temperatures.[8,9] The MCE is the property of some materials (like paramagnetic salts or magnetic stuffs) to get heated in the presence of magnetic field and cool down when the field is removed from the materials.[4] The compounds which show the sharp temperature-dependent magnetic-phase transition can have large MCE.[10] The magnetic cooling has several benefits against the gas refrigeration, such as low vibration, high efficiency, durability, and is environmental friendly. Therefore, in last decade more effort was done to develop the refrigerants with large MCE based on magnetic substances.

The physical properties of perovskite-type manganites can be changed by doping at A-site or B-site (Mn-site) with various elements having different ionic radii.[11,12] In manganites, doping with different elements alters the Mn^{3+}–O–Mn^{4+} network, which changes the strength of double exchange (DE) as well as superexchange interactions.[13] As compared to A-site doping, Mn-site doping will not only modify the Mn^{3+}–O–Mn^{4+} network but also brings about many complicated new magnetic exchange interactions between the Mn ions and doped transition metal ions.[14–16] The lattice effect, the concentration of Mn^{4+} ions, oxygen vacancies and the interaction of ferromagnetic DE or anti-ferromagnetic superexchange between the dopant and the Mn ions should be taken into account for Mn-site doping.[17,18] Due to this reason the Mn-site doping was performed in this work. It was found that dopant size and valence-induced local strain dominate the magneto-transport properties in manganites and change the long-range FM ordering; consequently change in the magnetic properties of the pervoskite manganites. In order to get the enhancement in the magnetocaloric response of the $La_{0.70}Ca_{0.1}Sr_{0.2}MnO_3$ (LCSMO) manganite, Fe was doped at Mn-site. The second goal of this research is to develop a potential refrigerant for magnetic cooling.

2. Experimental

The polycrystalline LCSMO and $La_{0.70}Ca_{0.1}Sr_{0.2}Fe_{0.1}Mn_{0.9}O_3$ (LCSFMO) samples were synthesized by using the solid-state reaction technique.[19] The metal oxide: La_2O_3, SrO, CaO, Fe_2O_3 and Mn_2O_3 (99.99% pure, Sigma-Aldrich) powders were mixed in stoichiometric amount using ethanol and were ball milled for 6 h. The mixed slurry was dried for 10 h at 80°C and then first heated at 800°C in air for calcination for 10 h. The dried powder was grinded and then pressed into a pellet shape. The pellets were first annealed at 1100°C for 30 h followed by repeated grinding.

*Author for correspondence (bhkoo@changwon.ac.kr, shafiqueamu@gmail.com)

Finally, the sintering of pellets was done at 1250°C for 24 h. The as-obtained pellets were used for characterization.

The polycrystalline behaviour and phase purity of the samples were studied by using a X-ray diffractometer (Bruker-D8-Advance) operating with $CuK_{\alpha 1}$ ($\lambda = 1.5406$ Å, 40 kV, 40 mA) radiation at room temperature. Scanning electron microscope (SEM; SEM-JSM5610) was used to study the surface morphology of the samples. Average grain size was determined by using the Image-J software from SEM micrographs. The magnetic measurements were recorded by using a vibrating sample magnetometer (PPMS-6000 VSM, Quantum design) with a temperature range of 4–400 K.

3. Results and discussion

The structural study of LCSFMO sample in terms of X-ray diffraction (XRD) pattern is shown in figure 1. The polycrystalline behaviour of the LCSFMO sample was observed from the XRD pattern with the multiple reflections. The rhombohedral structure ($R-3c$ space group) with the lattice constants of $a = b = 5.4981 \pm 0.005$ Å and $c = 13.2433 \pm 0.005$ Å was obtained for this sample using POWDER-X software. Also, the highest intensity was observed for the (104) plane as preferred orientation with rhombohedral structure. In order to compare, the XRD pattern of LCSMO is also plotted.

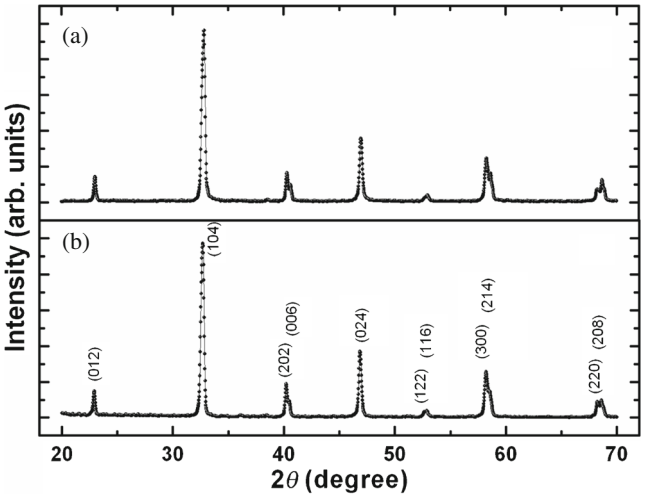

Figure 1. The XRD patterns of (**a**) $La_{0.7}Ca_{0.1}Sr_{0.2}MnO_3$ and (**b**) $La_{0.7}Ca_{0.1}Sr_{0.2}Fe_{0.1}Mn_{0.9}O_3$ samples.

Figure 2 shows the polycrystalline structure in typical SEM micrographs of the LCSFMO and LCSMO samples. It was observed that the both samples have mainly strongly connected grains. The LCSFMO sample has smaller grain size. The average grain size was found to ~9 and 6 μm for LCSMO and LCSFMO samples, respectively.

Figure 3a shows the magnetization of samples as a function of temperature. The magnetization measurement was performed in the temperature range of 100–375 K during the warming up cycle. The Curie temperature (T_C) was evaluated by determination of minimum of the derivative dM/dT of the M–T curve (not shown here). The obtained values of T_C are 232 and 350 K for LCSFMO and LCSMO samples, respectively. The lowering of T_C is because of the change in DE interaction in the LCSFMO sample created by Fe doping. On the other hand, ferromagnetism in Fe-doped sample is expected to enhance because of the Fe^{3+}–O–Mn^{3+} super-exchange interaction.[20] However, we observed negative contribution due to the weakening of DE interaction caused by Fe doping. From thermodynamics point of view, the presence of magnetic hysteresis in the working materials (magnetic refrigerants) has adverse effect on cooling efficiency. In that context, it is impressive to have the sample like LCSFMO because of no magnetic hysteresis (inset of figure 3b), which is benign for the cooling efficiency.

The magnetocaloric effect was evaluated by calculating the magnetic entropy change (ΔS_M) upon an application of magnetic field using the thermodynamic Maxwell's equation, given as follows:[21]

$$\Delta S_M(T, H) = S_M(T, H) - S_M(T, 0) = \int_0^H \left(\frac{\partial M}{\partial T}\right)_H dH. \quad (1)$$

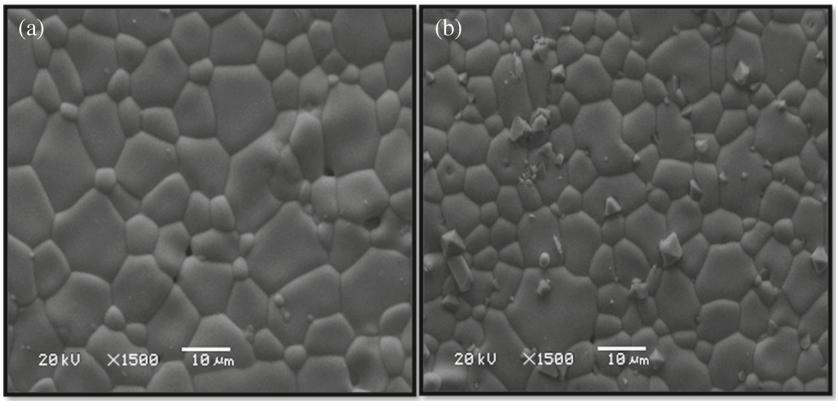

Figure 2. Scanning electron micrograph of (**a**) $La_{0.7}Ca_{0.1}Sr_{0.2}MnO_3$ and (**b**) $La_{0.7}Ca_{0.1}Sr_{0.2}Fe_{0.1}Mn_{0.9}O_3$ samples.

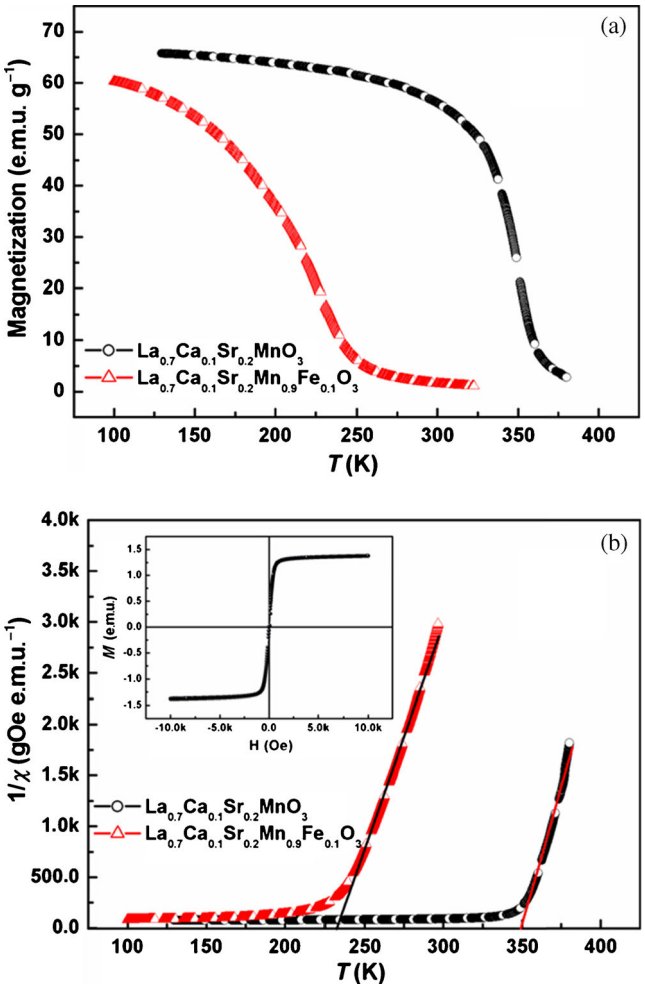

Figure 3. (**a**) Magnetization *vs.* temperature curve ($H = 0.5$ T) and (**b**) inverse magnetic susceptibility for $La_{0.7}Ca_{0.1}Sr_{0.2}MnO_3$ and $La_{0.7}Ca_{0.1}Sr_{0.2}Fe_{0.1}Mn_{0.9}O_3$ compounds. Inset is the M–H curve for $La_{0.7}Ca_{0.1}Sr_{0.2}Fe_{0.1}Mn_{0.9}O_3$ sample at 200 K.

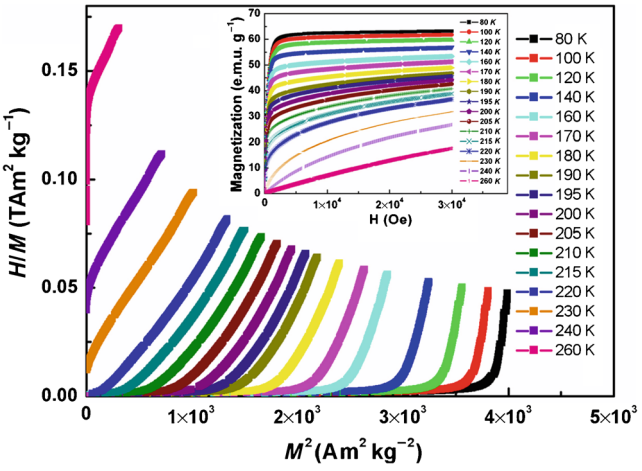

Figure 4. Arrott plots (H/M *vs.* M^2 isotherms). Inset is the magnetization *vs.* magnetic field curve for the $La_{0.7}Ca_{0.1}Sr_{0.2}Fe_{0.1}Mn_{0.9}O_3$ sample. The temperature of isotherms is indicated.

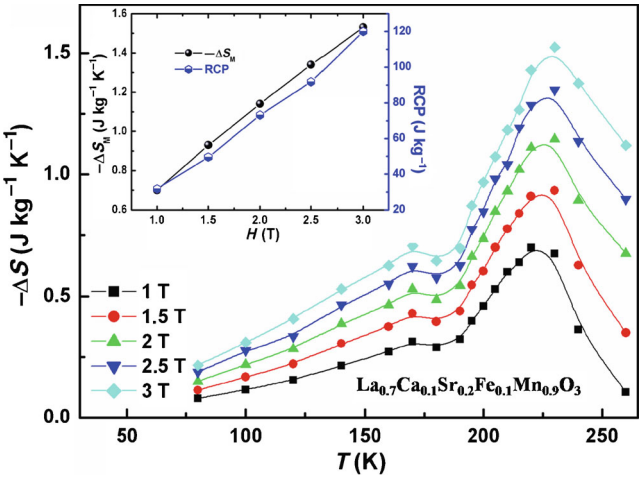

Figure 5. The ΔS_M of $La_{0.7}Ca_{0.1}Sr_{0.2}Fe_{0.1}Mn_{0.9}O_3$ sample at various magnetic fields. The inset is the $|\Delta S_M^{max}|$ and RCP values as a function of applied magnetic field.

The numerical approximation of equation (1) for magnetization measured at distinct field and temperature intervals is given as

$$-\Delta S_M(T, H) = \sum_i \frac{M_i - M_{i+1}}{T_{i+1} - T_i} \Delta H, \qquad (2)$$

where M_i and M_{i+1} are the magnitude of magnetization at the temperature T_i and T_{i+1}, respectively, under a magnetic field H_i. In our case, the minimum field was set to 0. Inset of figure 4 shows the evolution of magnetization with magnetic field (up to 3 T) at different temperatures on both sides of the T_C for LCSFMO sample. For accurate determination of maximum in magnetic entropy change ($|\Delta S_M^{max}|$), the different temperature interval was selected for different region (5 K near T_C and 10–20 K in other temperature regions). The increase in magnetization was observed with the decrease in temperature from 260 to 80 K, where more spins get aligned in the direction of field with decreasing temperature. The type of the magnetic phase transition in the LCSFMO sample has been investigated on the basis of the Banerjee criterion.[22] This criterion tells that at temperature higher than T_C, M^2 *vs.* H/M curves (Arrott plot) have positive and negative slopes for second- and first-order phase transition, respectively. A quintessential set of Arrott plots for the LCSFMO sample is depicted in figure 4. Clearly, the as-obtained Arrott plots show positive slope for all temperatures, i.e., the second order of phase transition.

The magnetic entropy change (ΔS_M) was determined numerically by using equation (2), for LCSFMO sample at different applied magnetic fields. Figure 5 shows that the LCSFMO sample has well enough $|\Delta S_M^{max}|$ as compared with other manganites.[10,23] Also, inset of figure 5 reveals that, the $|\Delta S_M^{max}|$ was found to increase deliberately with the magnetic field. The numerical values of $|\Delta S_M^{max}|$ at field change (ΔH) of 1 and 3 T were found ~0.71 and

1.53 J kg^{-1} K^{-1}, respectively. On the basis of this result, we conclude that the enhancement in $\left|\Delta S_{\mathrm{M}}^{\max}\right|$ is expected at higher applied magnetic fields.

The parameter, relative cooling power (RCP) plays a significant role in selection of good quality of refrigerants. It can be expressed as follows:[21]

$$\mathrm{RCP}(S) = \left|\Delta S_{\mathrm{M}}^{\max}\right| \times \partial T_{\mathrm{FWHM}}, \tag{3}$$

where $\partial T_{\mathrm{FWHM}}$ is the full-width at half-maximum and $\left|\Delta S_{\mathrm{M}}^{\max}\right|$ is the respective magnetic entropy change. The better magnetocaloric materials usually have large RCP values and consequently, have high cooling efficiency. Inset of figure 5 provides the information about RCP of the LCSFMO sample, also gives the behaviour of RCP against the applied magnetic field. The RCP value of 120 J kg^{-1} was observed for the field change (ΔH) of 3 T. One can notice that the higher magnetic field gives the larger RCP values for the same sample.

On the other hand, it is well understood that the magnetic refrigerants have good efficiency around the Curie temperature. In this regard, the magnetic refrigerants composed of materials having similar chemical and physical properties can facilitate wide range of working temperature as well as enhanced cooling efficiency. As the LCSFMO sample has the broad transition temperature and comparable RCP value, it can be used as potential magnetic refrigerants with a wide range of operating temperature.

4. Conclusions

We have made a precise analysis on magnetocaloric properties of complex LCSFMO compound. The polycrystalline LCSFMO manganite crystallized in the rhombohedral structure with preferred orientation of (104) plane. This compound exhibits considerably no magnetic hysteresis at 200 K, which is favourable for the magnetic cooling efficiency. A second order of transition from ferromagnetic to paramagnetic phase was observed. The improvement in the value of $\left|\Delta S_{\mathrm{M}}^{\max}\right|$ was found at higher magnetic field for the LCSFMO sample. The RCP value of 120 J kg^{-1} was observed for the ΔH of 3 T and increases with the applied magnetic field.

Acknowledgements

This research was supported by the Basic Science Research Program through the National Research Foundation of Korea (NRF) funded by the Ministry of Education, Science and Technology (2012-R1A1B3000784), and National Research Foundation of Korea (NRF) grant funded by the Korea government (MEST) (No. 2012-0009452).

References

1. Kumar P and Mahendiran R 2012 *Appl. Phys. Lett.* **101** 042411
2. Gschneidner Jr K A, Pecharsky V K and Tsokol A O 2005 *Rep. Prog. Phys.* **68** 1479
3. Anwar M S, Kumar S, Ahmed F, Arshi N and Koo B H 2012a *Mater. Res. Bull.* **47** 2977
4. Othmani S, Blel R, Bejar M, Sajieddine M, Dhahri E and Hlil E K 2009 *Solid State Commun.* **149** 969
5. Gschneidner Jr K A and Pecharsky V K 1999 *J. Appl. Phys.* **85** 5365
6. Pecharsky V K and Gschneidner Jr K A 1997 *Appl. Phys. Lett.* **70** 3299
7. Sarkar P, Mandal P and Choudhury P 2008 *Appl. Phys. Lett.* **92** 182506
8. Koubaa W C, Koubaa M and Cheikhrouhou A 2011 *J. Alloys Compd.* **509** 4363
9. Anwar M S, Kumar S, Ahmed F, Arshi N, Kim G W, Lee C G and Koo B H 2011 *J. Magn.* **16** 457
10. Anwar M S, Kumar S, Ahmed F, Heo S N, Kim G W and Koo B H 2013 *J. Electroceram.* **30** 46
11. Yang J, Song W H, Ma Y Q, Zhang R L, Zhao B C, Sheng Z G, Zheng G H, Dai J M and Sun Y P 2004 *Phys. Rev. B* **70** 092504
12. Anwar M S, Kumar S, Ahmed F, Arshi N and Koo B H 2012b *J. Nanosci. Nanotechnol.* **12** 5523
13. Hwang H Y, Cheong S W, Radaelli P G, Marenzio M and Batlogg B 1995 *Phys. Rev. Lett.* **75** 914
14. Mnefgui S, Zaidi N, Dhahri A, Hlil E K and Dhahr J 2014 *J. Solid State Chem.* **215** 193
15. Phan T L, Zhang P, Thanh T D and Yu S C 2014 *J. Appl. Phys.* **115** 17A912
16. Reshmi C P, Pillai S S, Suresh K G and Verma M R 2013 *Solid State Sci.* **19** 130
17. Troyanchuk I O, Bushinsky M V, Szymczak H, Baran M and Barner K 2007 *J. Magn. Magn. Mater.* **312** 470
18. De K, Majumdar S and Giri S 2007 *J. Phys.* **40** 5810
19. Anwar M S, Kumar S, Ahmed F, Hoon S C, Heo S N and Koo B H 2012c *J. Ceram. Process. Res.* **13** S100
20. Kanamori J 1959 *J. Phys. Chem. Solids* **10** 87
21. Thiyagarajan R, Muthu S E, Mahendiran R and Arumugam S 2014 *J. Appl. Phys.* **115** 043905
22. Banerjee S K 1964 *Phys. Lett.* **12** 16
23. Ehsani M H, Kameli P, Ghazi M E, Razavi F S and Taheri M 2013 *J. Appl. Phys.* **114** 223907